

Mechanism for excimer-laser ablation in alkaline-earth metals

Hiroaki Nishikawa* and Masaki Kanai

The Institute of Scientific and Industrial Research, Osaka University, 8-1 Mihogaoka, Ibaraki, Osaka 567-0047, Japan

Gabor Szabo

Department of Optics and Quantum Electronics, JATE University, Dom ter 9, Szeged 6720, Hungary

Tomoji Kawai

The Institute of Scientific and Industrial Research, Osaka University, 8-1 Mihogaoka, Ibaraki, Osaka 567-0047, Japan

(Received 16 April 1999)

The time-of-flight distribution and the amount of desorbed monovalent ion were measured for laser ablation of alkaline-earth metals. The experiment is performed using two wavelengths (193-nm ArF excimer laser and 248-nm KrF excimer laser), a fluence of less than 500 mJ/cm² and an effective pulse duration of 14–20 ns. Ion desorption occurs at a lower fluence than that predicted by a thermal evaporation model. The relationship between the amount of desorbed ion and the fluence shows highly nonlinear behavior. Based on the obtained results, a model is proposed in which the laser ablation of alkaline-earth metals is caused by the core electron ionization via the multiphoton photochemical process.

I. INTRODUCTION

The ultraviolet (UV) laser ablation mechanism, which consists of an interaction between condensed matter and photons, is a new subject of study in the field of photochemistry. During the past decade, study of the fundamental processes of laser ablation has been insufficient, due in part to the success of applications of thin-film formation as a pulsed laser deposition (PLD) technique. However, further progress in the optimization and control of PLD techniques that will enable the quality of the deposited films to be improved requires a greater knowledge of the underlying fundamental phenomena that govern laser ablation. As a result, the number of studies examining the ablation mechanism has increased. Such studies are complicated because laser ablation is a transient process involving complex physics and depends on several parameters such as the wavelength, pulse duration, and fluence of the laser beam and the material irradiated by the laser, i.e., the *target*. Since laser ablation involves the local breaking of chemical bonds, the process is thought to be strongly dependent on the nature of the chemical bond. Thus the characteristics of the bond of the target material is thought to have the greatest effect on the mechanism of laser ablation.

Chemical bonds can be classified into three types: ionic bond crystal, covalent bond crystal, and metallic bond crystal. A reliable model has already been proposed for the first two types of chemical bond.^{1–5} In these crystals, the nascent process of laser ablation has been concluded to be not simple thermal evaporation, but rather the electronic excitation mechanism. The essential requirement in these models is the localization of the electronic excited state. The mechanism for the metallic bond crystal, however, is not well understood compared with the other crystals. In general, the laser ablation of metal is thought to be caused by the thermal process.⁶ Several thermal mechanisms have been proposed including thermal evaporation,⁷ exfoliation sputtering with thermal

shock,⁸ and the hydrodynamic process with thermal melting.⁸ In previous models, the first stage of the ablation is considered to be free-electron acceleration by the absorption of photons via the inverse bremsstrahlung process.^{6,7,9} The accelerated electrons collide with the lattice and excite the phonon with the time scale of a few ps.^{6,7,9} The energy injected into the electronic system is transferred to the lattice system within picoseconds. Absorption of UV light is not so effective for metals,^{10,11} because the plasma cutoff frequency for almost all metals is in the UV region, i.e., the metallic bond crystal transmits the UV laser.¹² As a result, a large fluence is required for metal ablation⁷ in order to heat the surface region above the melting point. However, ablation has been reported to occur at very low fluence,¹³ which cannot heat the surface region beyond the melting point. Therefore the laser ablation mechanism of metal is not a simple thermal evaporation process.

In order to clarify the process of laser ablation for metals, a systematic investigation of the laser ablation of three alkaline-earth metals, Ca, Sr, and Ba, was performed. The metals in this group have similar chemical characteristics, so systematic evaluation is possible by comparison of the experimental results. In the present study, time-of-flight (TOF) distribution and the amount of monovalent ion desorbed by the laser ablation of the alkaline-earth metals are investigated using a time-resolved quadrupole mass spectrometer (QMS) using two wavelengths and various values of fluence. Furthermore, the effective pulse duration is varied using a double pulsed laser ablation technique in order to study the time scale of the process. Based on the experimental results, a different model is proposed for the laser ablation mechanism of metals.

II. EXPERIMENT

A schematic diagram of the experimental apparatus is shown in Fig. 1(a). Measurement of the desorbed monova-

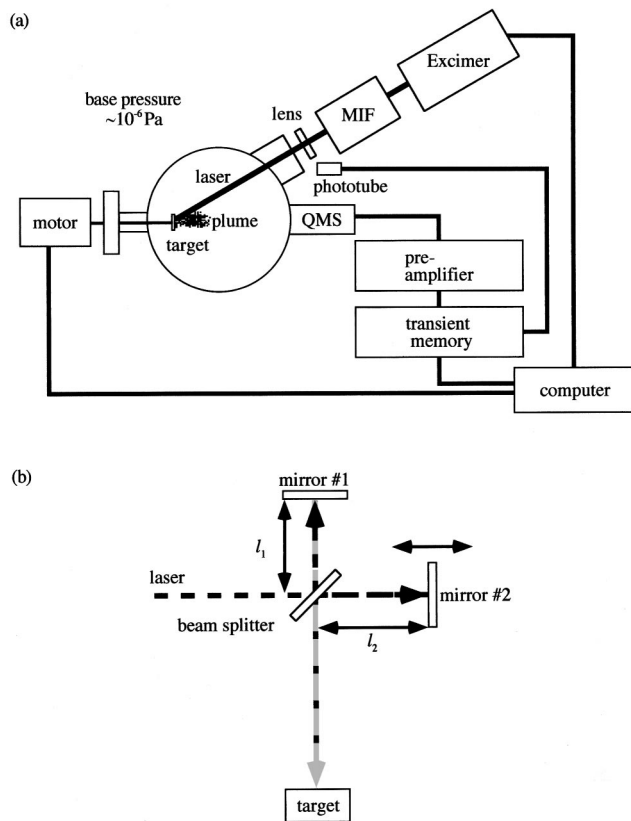


FIG. 1. (a) Schematic diagram of the laser ablation experiments. (b) Sketch of Michelson interferometer producing two ablation pulses having various delays.

lent ion was performed in a vacuum chamber with a base pressure of 2×10^{-8} mbars. Plates of Ca, Sr, and Ba (rare metallic: polycrystalline with a purity of 99%) placed in the chamber were irradiated either by an ArF excimer laser (Lumonics: EXCIMER-700, $\lambda = 193$ nm, full width at half maximum (FWHM) of each pulse = 14 ns) or by a KrF excimer laser (Lambda Physics: COMPEX-102, $\lambda = 248$ nm, FWHM of each pulse = 14 ns). The laser pulse was focused onto the target by an artificial silica lens with a focal length of 4.4×10^2 mm (spot size of the focused beam on the target was 2.0×0.7 mm²). The oxide layers on the plate surfaces were removed by preablation in the vacuum chamber before the measurements were performed. The desorbed ions were detected by a QMS (VG Gas Analysis: SXP300). The distance between the target and the QMS was 5.4×10^2 mm. The QMS signal was amplified by a preamplifier (NF Electronic Instruments: 5305, frequency response = dc \sim 10 MHz) and then stored in a transient memory device (Kawasaki Electronica: MR-50E) having a sampling rate of 400 ns. The zero point of the time axis was determined using a phototube (Hamamatsu Photonics: R1826, applicable for the wavelength region of 185 \sim 320 nm, response is faster than 1 ns) placed near the focusing lens. The time delay between the phototube signal and target irradiation is negligible when the sampling rate is 400 ns. The sample was rotated between each laser shot by a stepping motor in order to ensure that the ablation was always performed on a fresh surface.

Double pulsed laser ablation was achieved by applying two laser pulses separated by various delay times. The two

pulses were obtained by producing two replicas of a single laser pulse by a Michelson interferometer (MIF) inserted between the excimer laser and the focusing lens [see Fig. 1(b)]. This technique enables us to vary the effective pulse duration without changing the total fluence. The fluence of each pulse was 200 mJ/cm² at the target surface (i.e., the total fluence was 400 mJ/cm²). The position of one of the mirrors (no. 1) was fixed, and the other mirror was mounted on an optical rail having a maximum traveling distance of 1 m, which corresponds to a maximum delay of about 6 ns between the two pulses.

In this experiment, special care was taken to ensure that only the delay between two pulses was changed while all other parameters remained constant. By alternately blocking one of the laser paths of the MIF, the pulses traveling along each path were confirmed to produce the same QMS signal. In order to prevent errors due to energy loss and focal-spot diameter changes due to the change in the optical path of the delayed arm, the QMS signal produced by the beam from the moving mirror was confirmed to show no measurable dependence on mirror position. The position of the focal spots of the beam from each arm has the potential for being the source of the most serious error. Therefore the deviation of the focal points of the two laser beams was eliminated for all mirror positions by consistently realigning the optical system. The realignment was accomplished with the aid of a pinhole having a diameter of about 1 mm which was set in front of the beam splitter of the MIF. Using the above-mentioned procedure, the lateral deviation of the two laser beams at the target surface was less than 5×10^{-2} mm. This value is the smallest scale of the ruler used in the experiment.

III. RESULTS AND DISCUSSION

A. TOF spectra and the amount of desorbed monovalent ion

Figures 2 and 3 show the TOF spectra of the monovalent ion desorbed by the ArF excimer laser ablation of Ca, Sr, and Ba. The result indicates that the metal ablation is not a simple thermal process. The ion desorption in the fluence region below 200 mJ/cm² cannot be explained by simple thermal evaporation. In the thermal evaporation model, the ion desorption is believed to occur at a fluence of greater than about 1 J/cm².^{7,14}

The solid lines in Figs. 2 and 3 are theoretical curves obtained using the following Maxwell-Boltzmann distribution, which is corrected by center-of-mass velocity:¹⁵

$$n(t) = At^{-4} \exp[-m(z/t - v_g)^2 / 2k_B T]. \quad (1)$$

Here, $n(t)$ represents the ion flux observed at time t , A is a normalization constant, m is the mass of the ion, z is the distance from the target to the QMS, v_g is the center-of-mass velocity, k_B is Boltzmann's constant, and T is the temperature: v_g and T are used as adjustable parameters. The results show good agreement with Eq. (1) at a laser fluence of less than 190 mJ/cm² [Fig. 2(a)], 190 mJ/cm² [Fig. 2(b)], and 90 mJ/cm² [Fig. 2(c)] for Ca⁺, Sr⁺, and Ba⁺, respectively. This indicates that the desorbed ions reach thermal equilibrium. Such equilibrium will result from frequent collisions between the ions at the initial stage of the ablation when the ion density is very high. However, at fluences higher than those

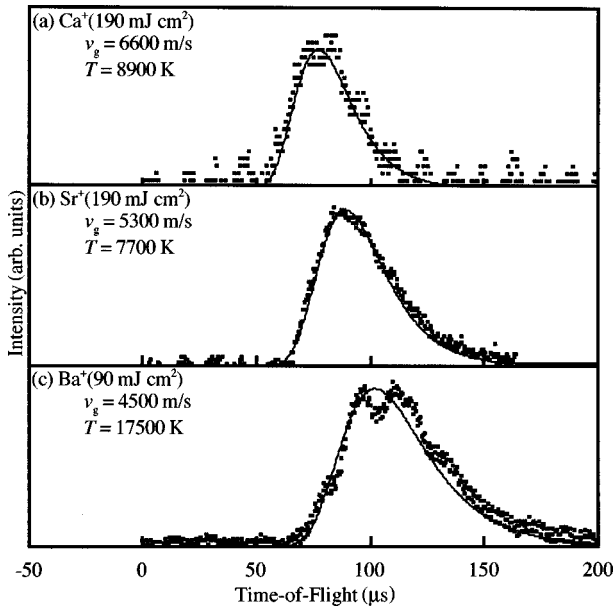


FIG. 2. TOF spectra of Ca^+ , Sr^+ , and Ba^+ desorbed by ArF excimer laser ablation. Laser fluence is (a) 190 mJ/cm^2 , (b) 190 mJ/cm^2 , and (c) 90 mJ/cm^2 . The solid lines are the theoretical curves obtained using the Maxwell-Boltzmann distribution corrected by center-of-mass velocity. Adjustable parameters are (a) $v_g = 6600 \text{ m/s}$ and $T = 8900 \text{ K}$, (b) $v_g = 5300 \text{ m/s}$ and $T = 7700 \text{ K}$, and (c) $v_g = 4500 \text{ m/s}$ and $T = 17500 \text{ K}$. The TOF spectra show good agreement with the Maxwell-Boltzmann distribution.

listed above, the TOF spectra deviate from the Maxwell-Boltzmann distribution (Fig. 3), and higher fluence results in larger deviation. This deviation is thought to be caused by the generation of delayed components. Namely, higher than critical fluence may produce ions deep inside the solid, which causes a time delay because those ions collide with the chemical species desorbed from the surface region.

Figure 4 shows the relationship between the effective temperature of the desorbed monovalent ion and the fluence of the ArF excimer laser. The graph is plotted for the region in which the measured TOF spectra agree with Eq. (1), i.e., the region in which the Maxwell-Boltzmann distribution is corrected by center-of-mass velocity. The temperature in Fig. 4 is higher than that predicted by the thermal evaporation model.^{7,14} These results also indicate that laser ablation of metal does not occur as simple thermal evaporation.

As shown in Fig. 4, the temperature is proportional to the fluence (I). This linear behavior can be explained by a model in which the source of the thermal energy is the later part of the laser beam. In this model, the photon which remains incident after the desorption is absorbed by the free electron in the plume via the inverse bremsstrahlung process.¹⁶ The accelerated electron can interact with the ion or neutral species, namely the absorbed energy is redistributed among all desorbed chemical species.^{7,14} This results in an increase in the kinetic energy of desorbed chemical species. Thus the energy absorbed into the plume is thought to correspond to the thermal energy. The absorbed energy is assumed to be proportional to the fluence,¹² so the redistributed energy is also proportional to I . In this manner, the temperature is shown to be proportional to the fluence.

Figures 5 and 6 show the amount of desorbed ion vs the

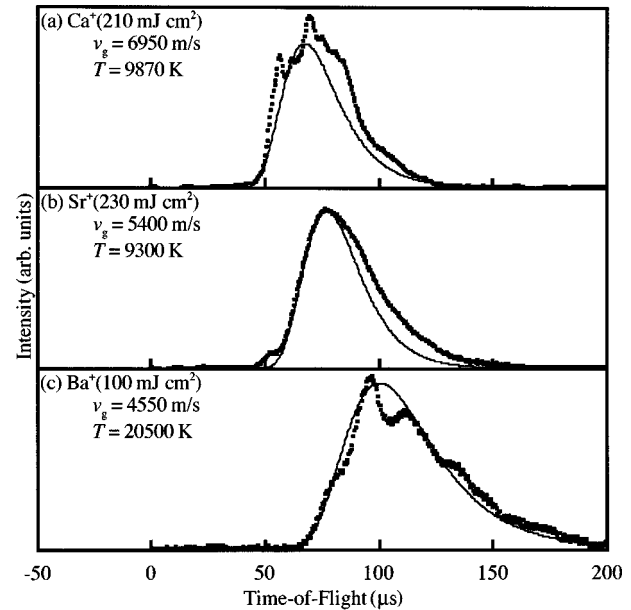


FIG. 3. TOF spectra of Ca^+ , Sr^+ , and Ba^+ desorbed by ArF excimer laser ablation. Laser fluence is (a) 210 mJ/cm^2 , (b) 230 mJ/cm^2 , and (c) 100 mJ/cm^2 . The solid lines are the theoretical curves obtained using the Maxwell-Boltzmann distribution corrected by center-of-mass velocity. Adjustable parameters are (a) $v_g = 6950 \text{ m/s}$ and $T = 9870 \text{ K}$, (b) $v_g = 5400 \text{ m/s}$ and $T = 9300 \text{ K}$, and (c) $v_g = 4550 \text{ m/s}$ and $T = 20500 \text{ K}$. In the fluence region higher than that shown in Fig. 2, the TOF spectra show deviation from the Maxwell-Boltzmann distribution.

fluence for the ArF excimer laser and the KrF excimer laser, respectively. The amount of desorbed ion is obtained by the integration of each TOF spectrum. For Ca^+ , Sr^+ , and Ba^+ , respectively, the amount of desorbed ion is found to be proportional to $I^{4.6 \pm 0.2}$, $I^{3.7 \pm 0.4}$, and $I^{2.9 \pm 0.3}$ by the irradiation of

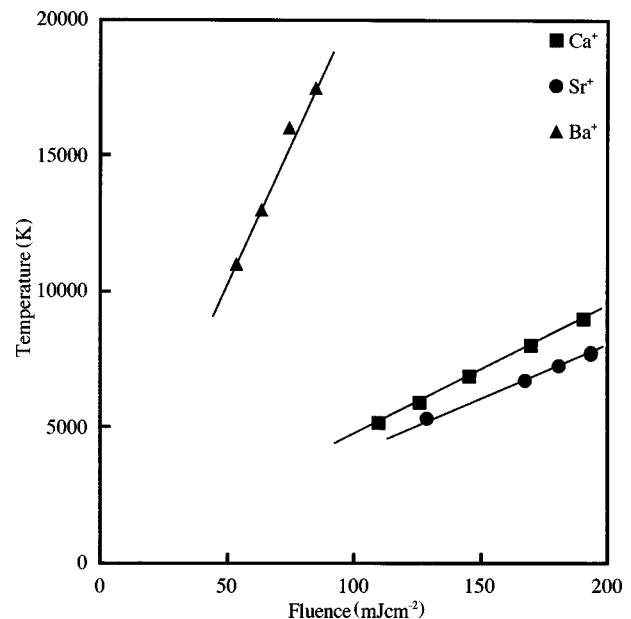


FIG. 4. The relationship between the temperature of the desorbed ion and the laser fluence for ArF excimer laser ablation of Ca, Sr, and Ba. The temperature is proportional to the fluence for all elements.

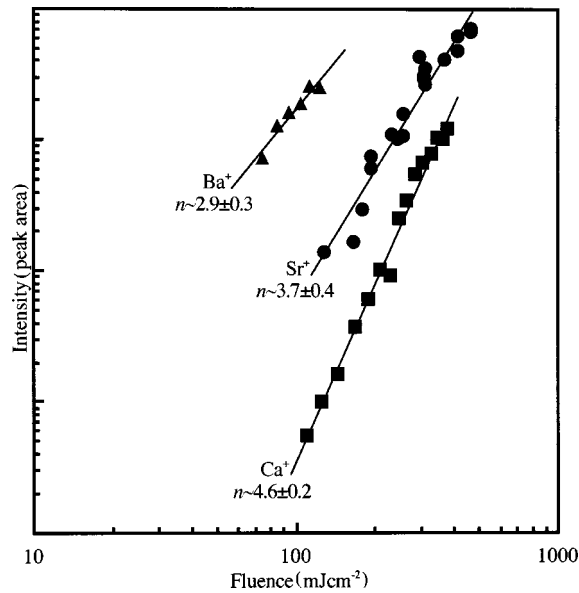


FIG. 5. Amount of monovalent ion vs. fluence using ArF excimer laser. Both axes are logarithmic scales. Each amount is obtained by integrating the TOF spectrum. The amount of desorbed ion is found to be proportional to $I^{4.6 \pm 0.2}$, $I^{3.7 \pm 0.4}$, and $I^{2.9 \pm 0.3}$ for Ca^+ , Sr^+ , and Ba^+ , respectively. Here, I represents the fluence.

ArF excimer laser. The result for the KrF excimer laser are $I^{6.4 \pm 1.0}$, $I^{5.3 \pm 1.2}$, and $I^{3.6 \pm 1.0}$ for Ca^+ , Sr^+ , and Ba^+ , respectively. In the thermal evaporation model, the amount of desorbed neutral atom will be roughly proportional to $(I - I_{\text{th}})$, where I_{th} is the threshold fluence that is equal to the energy required for the surface heating to either the melting point or boiling point.¹⁷ This simple consideration is based on the fact that the surface temperature will be proportional to the injected energy. Therefore the nonlinear behavior seen in Figs. 5 and 6 cannot be explained by the simple thermal

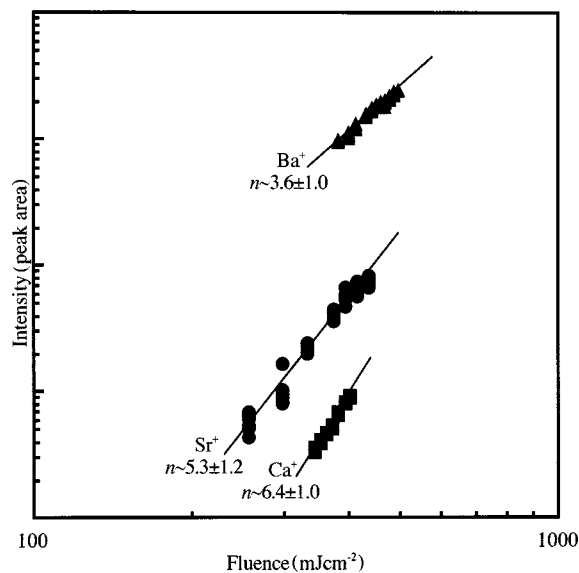


FIG. 6. Amount of monovalent ion vs. fluence using KrF excimer laser. Both axes are logarithmic scales. Each amount is obtained by integrating the TOF spectrum. The amount of desorbed ion is found to be proportional to $I^{6.4 \pm 1.0}$, $I^{5.3 \pm 1.2}$, and $I^{3.6 \pm 1.0}$ for Ca^+ , Sr^+ , and Ba^+ , respectively.

TABLE I. The binding energies of the highest core electron measured from the vacuum level and the total photon energies obtained experimentally, i.e., the sum of five-, four- and three-photon energies of the ArF excimer laser and the sum of six-, five- and four-photon energies of the KrF excimer laser.

Orbital	Binding energy/eV	Photon energies for ArF /eV (6.4 eV/photon)	Photon energies for KrF /eV (5.0 eV/photon)
Ca 3p	27.7	32	30
Sr 4p _{3/2} , 4p _{1/2}	22.7, 23.8	25.6	25
Ba 5p _{3/2} , 5p _{1/2}	16.9, 19.1	19.2	20

evaporation model. Since the power law can be interpreted as a multiphoton photochemical reaction, the desorption of monovalent ion may be caused by five, four, and three photon processes when using an ArF excimer laser of 6.4 eV/photon, for Ca^+ , Sr^+ , and Ba^+ , respectively. Likewise, the desorption of monovalent ion may be caused by six-, five-, and four-photon processes when using a KrF excimer laser of 5.0 eV/photon for Ca^+ , Sr^+ , and Ba^+ , respectively. Based on these results, another model is constructed for the nascent process of the laser ablation of metal on the premise that the direct electronic process is important. First, the excitation of the band electron is discussed. In the typical metal, the band electron does not absorb UV light effectively.¹¹ In fact, the absorption coefficient is $\sim 10\%$ for a typical metal at the UV region.¹² Furthermore, only one photon is sufficient for the excitation of the band electron above the vacuum level, because the work function of the alkaline-earth metal¹⁸⁻²⁰ is lower than 5.0 eV. This contradicts the experimental results. Therefore the excitation of the core electron is discussed. Table I shows the binding energies of the highest core electron measured from the vacuum level¹⁸⁻²¹ and the total photon energies shown by the experimental results, i.e., five-, four-, and three-photon energies of the ArF excimer laser and six-, five-, and four-photon energies of the KrF excimer laser. These photon energies are found to slightly exceed the binding energies of the highest core electron. The completely systematic result proposes a model in which the nascent process of ion desorption in the laser ablation of the alkaline-earth metal is the ionization of the highest core electron. The power law in Figs. 5 and 6 cannot be explained in terms of the core ionization after the neutral atom desorption. For the desorption of the neutral atom, at least one photon is required. Since the potential energy of the core electron in the neutral atom is close to that in the solid-state crystal, the photon number used for core electron ionization by the multiphoton process is identical. Namely, the mechanism of neutral desorption followed by the core electron ionization of atomic species requires an additional photon.

The TOF spectra and the amount of desorbed monovalent ion were measured for the laser ablation of the alkaline-earth metal using time-resolved QMS. The ion is desorbed in the fluence region by less than several hundred mJ/cm^2 , but the simple thermal evaporation mechanism cannot predict ion desorption having such a low fluence. The temperature obtained from the fitting of the TOF spectra to the Maxwell-Boltzmann distribution corrected by the center-of-mass velocity is much higher than that obtained by the prediction of

the thermal evaporation model. The amount of desorbed monovalent ion is proportional to I^n where $n > 1$. These results prove that the ablation of alkaline-earth metals does not occur by simple thermal evaporation. The power law can be consistently interpreted as the highest core electron ionization by the multiphoton photochemical reaction. Therefore the multiphoton process is thought to be the trigger of the ablation for alkaline-earth metals.

B. Effect of the variation of the effective pulse duration by the double pulsed laser ablation technique

In the previous section, a model was proposed for the laser ablation of the metallic bond crystal, i.e., the core electron excitation by the multiphoton process. At this point, however, the proposed model is considered to be somewhat tentative, and further experimental evidence is needed. One of the key points is to clarify the role of the thermal and nonthermal (electronic) phenomena in the ion desorption. We should note that the time scale of the thermal and electric phenomena is different. The thermal evaporation mechanism normally has a time scale of around 10 ns or longer at the fluence region below about 1 J/cm^2 ,⁷ whereas the electronic process is on an order of less than 1 ns. The amount of desorbed chemical species is sensitive to the duration of the laser pulse if the photochemical process plays an important role in the ablation phenomenon. Thus the variation of the laser pulse duration is an effective means by which to verify the proposed model.

In order to perform the present study, the double pulsed laser ablation technique is used. In this technique, the time profile of the laser beam is controlled using the delay time between two pulses. In other words, the effective pulse width and the photon number per unit time can be changed. The relationship between the delay time and the amount of desorbed Ca^+ is examined. Based on the results, the time scale of the process is discussed.

In Fig. 7, the squares indicate the measured dependence of the amount of desorbed Ca^+ on the delay time. The amount of desorbed ion was obtained by the integration of the TOF spectra for each delay time. The ordinate in Fig. 7 is the ratio of the signal intensity to that of the single pulse ablation. On the simple assumption that the fifth-order process is responsible for the ion desorption, the amount of the ion is expected to be proportional to the fifth power of the light intensity, i.e.,

$$n(\Delta t) \propto \int_{-\infty}^{\infty} [I(t) + I(t - \Delta t)]^5 dt. \quad (2)$$

Here, $I(t)$ is the time profile of the single laser pulse and Δt is the delay between the two pulses. The time profile of the laser intensity for the single pulse is shown in Fig. 8 (the intensity scatter in the digitized experimental data causes the numerical variation in the evaluation of Eq. (2), thus the analytical fit of $I(t) \propto t^{2.2} \exp(-0.335t)$ indicated by the solid line in Fig. 8 was used for the calculation). The behavior expected from Eq. (2) is represented by the dashed line in Fig. 7. Comparing the dashed line to the measured data reveals that the decrease in the amount of desorbed ion due to the increase of Δt is faster than that expected from Eq. (2). The amount of ion drops by approximately one order of

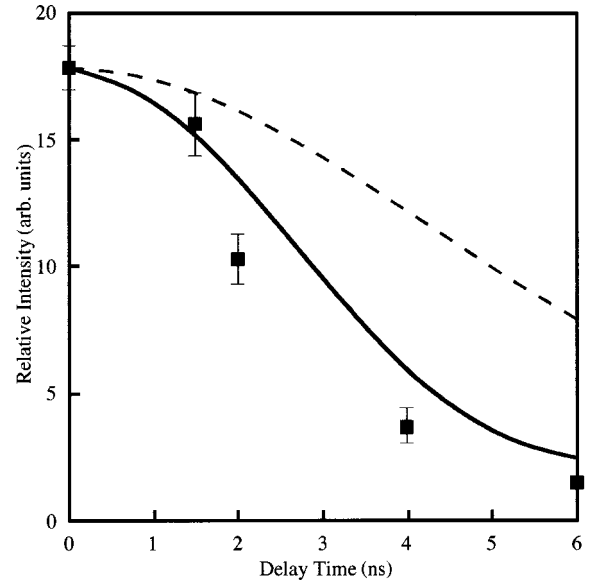


FIG. 7. Measured dependence of the amount of desorbed Ca^+ on the delay time between the two ablating laser pulses (squares) for ArF excimer laser ablation of Ca metal. The ordinate shows the ratio of the value of the signal to that of the single pulse ablation. The solid line is the best-fit line calculated using Eqs. (3) and (4) (see text), and the dashed line is obtained under the assumption of a five-photon process only, i.e., Eq. (2).

magnitude at a delay of 6 ns. The following explanation is suggested for this phenomenon. The chemical species is assumed to be desorbed until the plasma formation on the target surface, that is, when the energy deposited into the metal reaches a certain threshold value (E_0), the ablation suddenly stops. Since the plasma formed on the surface can absorb or reflect laser light, the plasma screens the target surface from the laser beam. Based on this assumption, the amount of the ion can be calculated as

$$n(\Delta t) \propto \int_{-\infty}^{\tau} [I(t) + I(t - \Delta t)]^5 dt. \quad (3)$$

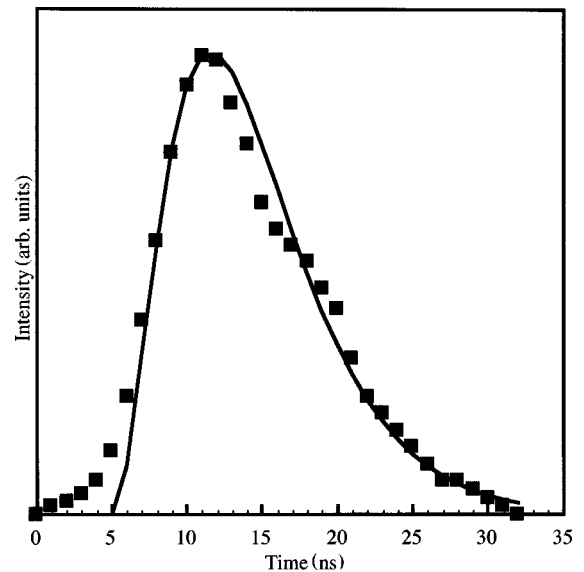


FIG. 8. Time profile of the experimental laser pulse (squares) and the analytical fit used for the calculation (solid line).

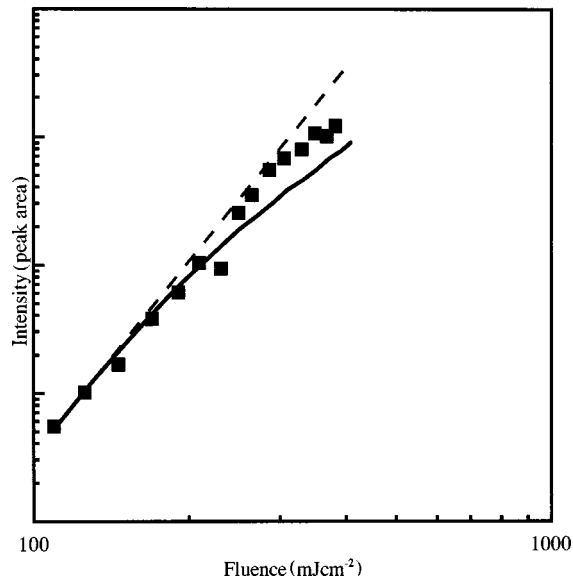


FIG. 9. Relationship between the amount of Ca^+ and the fluence for the simple ablation condition using an ArF excimer laser for Ca metal (squares). The dashed line shows the simple five-photon process and the solid line shows the relationship calculated using Eqs. (3) and (4) for single pulse ablation. The experimental results at higher fluence are closer to the solid line than the dashed line.

The τ can be obtained by evaluating

$$E_0 = \int_{-\infty}^{\tau} [I(t) + I(t - \Delta t)] dt. \quad (4)$$

The solid line in Fig. 7 is drawn based on Eqs. (3) and (4) using E_0 as a fitting parameter [note that the only unknown parameter in Eqs. (3) and (4) is E_0]. The best-fit line, i.e., the solid line shown in Fig. 7, is obtained with $E_0 = 0.19E$, where E is the total energy of the laser passing through the MIF. In this experiment, E corresponds to the total fluence of 400 mJ/cm^2 . The absolute value of E_0 can be calculated to be about 80 mJ/cm^2 . As Fig. 7 shows, the agreement between the calculation and the measured data is satisfactory. The laser ablation of Ca metal using the ArF excimer laser is thought to terminate when the injected energy reaches about 80 mJ/cm^2 . This value corresponds to a duration of a few ns for the time profile of the laser, i.e., the surface decomposition during the ablation process occurs only at the first several ns of the laser. Thus the time scale of the surface decomposition should be of ns order, i.e., this result indicates that the ablation is not a simple thermal process. The later part of the laser beam should not contribute to the decomposition because this part is considered to be screened by the plasma formed on the target, as assumed above. This model is consistent with the discussion in the previous section. In Sec. III A, the temperature of the plume originated in the later part of the laser beam, which is absorbed by the free electron in the plume via the inverse bremsstrahlung process. Namely, the later part of the laser is not absorbed by the target, but rather by the free electrons in the plume.

This model modifies the relationship between the amount of the desorbed Ca^+ and the fluence from the simple five-photon process in the case of a single laser beam. In Fig. 9, the relationship calculated using Eqs. (3) and (4) is shown

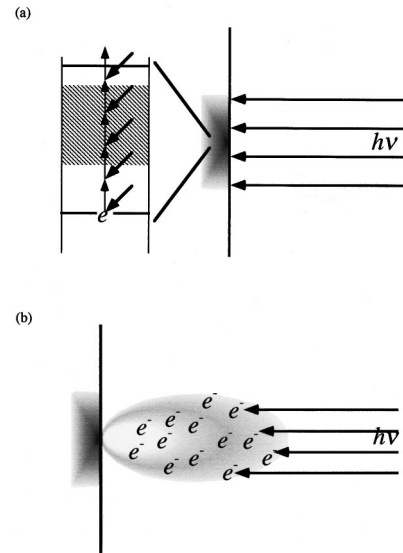


FIG. 10. Schematic illustration of the laser ablation mechanism of alkaline-earth metals. (a) The core electron is excited by the multiphoton process. (b) The laser beam is cut off by the inverse bremsstrahlung process of the electrons included in the plume. The energy injected into the electron system is redistributed into the entire chemical species by collision or Coulomb force.

for the single laser beam. The calculation shows better agreement with the experimental results, i.e., the higher fluence of the measured data deviates from the simple five-photon process.

The double pulsed laser ablation technique was performed in order to study the time scale for the phenomena on Ca metal for an ArF excimer laser. The amount of the desorbed Ca^+ is measured using a QMS as a function of the delay between two laser pulses. In the case of the irradiation of equivalent laser pulses with a 6-ns delay, the amount of desorbed Ca^+ is drastically decreased compared to that without the delay. The total amount of desorbed Ca^+ was quantitatively analyzed as a function of the delay time based on the results presented in a previous section, i.e., the five-photon process. The experimental results are proven to be clarified by introducing a model in which the laser is cutoff at the threshold fluence. The Ca^+ are found to be desorbed by only the early part of the laser pulse and the ion desorption terminates before the pulse is over. Ion desorption finishes at the time scale of less than several ns. The termination of the ion desorption is thought to be due to the screening of the laser by the plasma on the target surface. This consideration is consistent with the model in the previous section. The source of the plume temperature is supplied via the absorption of the laser energy by free electrons in the plume.

C. Synthetic model of ablation for alkaline-earth metal

The mechanism of laser ablation for alkaline-earth metals was discussed in the previous two sections based on systematic experimental results. The synthetic model is now summarized in this section for the phenomena, as shown in Fig. 10.

The first process of the phenomenon is the highest core electron ionization by multiphoton process [Fig. 10(a)]. This is the trigger of the surface decomposition. Since the absorp-

tion cross section of the photochemical process with three or more photons is nearly 0 for the excitation via virtual states, the excitation path should be real state, but details are not revealed in the present study. The second process of the phenomenon is the screening of the later part of the laser by free electrons in the plume [Fig. 10(b)]. Since the free electrons absorb the photon via inverse bremsstrahlung process, the laser beam cannot arrive at the target surface. In other words, the energy of the laser is injected into the plume and the surface decomposition is stopped. The energy injected into the free electrons in the plume is redistributed into the entire chemical species in the plume by collision or Coulomb force resulting in the realization of the thermal equilibrium state. For this reason, the Maxwell-Boltzmann-type TOF spectra are observed to be above more than several thousand K.

IV. CONCLUSIONS

In conclusion, laser ablation of alkaline-earth metals has been investigated in an attempt to understand the nascent process of metal ablation. The TOF spectra and the amount

of desorbed monovalent ion have been measured using ArF and KrF excimer laser as light sources. The ion is desorbed with a fluence of less than several hundred mJ/cm^2 . The relationship between the amount of desorbed ion and the fluence shows highly nonlinear behavior. Based on these results, a model has been proposed for metal ablation, whereby laser ablation of alkaline-earth metals is caused by ionization of the highest core electron via the multiphoton photochemical reaction. Double pulsed laser ablation has been performed in order to study the time scale for the phenomena on Ca metal using an ArF excimer laser. The total amount of desorbed Ca^+ has been quantitatively analyzed as a function of the delay time based on the multiphoton process. The experimental result is understood by introducing a model in which the laser absorption is cut off at a certain threshold fluence and the Ca^+ are desorbed only during the early part of the laser pulse. The termination of the ion desorption is thought to be due to the screening of the laser by the plasma on the target surface. Based on the obtained results, the synthetic model has been proposed for the laser ablation of alkaline-earth metals.

*Present address: Department of Electronic System and Information Engineering, Faculty of Biology-Oriented Science and Technology, Kinki University, 930 Nishi-Mitani, Uchita, Naga, Wakayama 649-6493, Japan.

¹M. L. Knotek and P. J. Feibelman, *Phys. Rev. Lett.* **40**, 964 (1978).

²M. L. Knotek, *Phys. Today* **37** (9), 24 (1984).

³R. L. Webb, L. C. Jensen, S. C. Langford, and J. T. Dickinson, *J. Appl. Phys.* **74**, 2323 (1993).

⁴N. Itoh and T. Nakayama, *Phys. Lett. A* **92**, 471 (1982).

⁵R. F. Haglund, Jr., in *Laser Ablation: Mechanisms and Applications—II*, Proceedings of the Second International Conference on Laser Ablation, edited by J. C. Miller and D. B. Geohegan, AIP Conf. Proc. No. 288 (AIP, New York 1994), p. 335.

⁶N. Bloembergen, in *Laser Ablation: Mechanisms and Applications—II*, Proceedings of the Second International Conference Laser Ablation (Ref. 5), p. 3.

⁷A. Vertes, R. W. Dreyfus, and D. E. Platt, *IBM J. Res. Dev.* **38**, 3 (1994).

⁸R. Kelly, J. J. Cuomo, P. A. Leary, J. E. Rothenberg, B. E. Braren, and C. F. Aliotta, *Nucl. Instrum. Methods Phys. Res. B* **9**, 329 (1985).

⁹J. C. S. Cools, *Pulsed Laser Deposition of Thin Films*, edited by

D. B. Chrisey and G. K. Hubler (Wiley, New York, 1994), p. 455.

¹⁰I. Lee, J. E. Parks II, T. A. Callcott, and E. T. Arakawa, *Phys. Rev. B* **39**, 8012 (1989).

¹¹L. K. Ang, Y. Y. Lau, R. M. Gilgenbach, and H. L. Spindler, *Appl. Phys. Lett.* **70**, 696 (1997).

¹²C. Kittel, *Introduction to Solid State Physics*, 6th ed. (Wiley, New York, 1986), Chap. 10, p. 259.

¹³H. Helvajian and R. Welle, *J. Chem. Phys.* **91**, 2616 (1989).

¹⁴R. W. Dreyfus, *J. Appl. Phys.* **69**, 1721 (1991).

¹⁵J. P. Zheng, Z. Q. Huang, D. T. Shaw, and H. S. Kwock, *Appl. Phys. Lett.* **54**, 280 (1989).

¹⁶R. K. Singh and J. Narayan, *Phys. Rev. B* **41**, 8843 (1990).

¹⁷J. J. Dubowski (private communication).

¹⁸K. A. Kress and G. J. Lapeyre, *Solid State Commun.* **9**, 827 (1971) (Ca: $\Phi=2.9$ eV).

¹⁹L. Gault, P. Renucci, and R. Rivoira, *Phys. Rev. B* **15**, 3078 (1977) (Sr: $\Phi=2.64$ eV).

²⁰L. Gault, P. Renucci, and R. Rivoira, *J. Appl. Phys.* **49**, 4105 (1978) (Ba: $\Phi=2.3$ eV).

²¹The energy difference between the core electron level and Fermi level was measured by x-ray photoelectron spectroscopy. The data are shown in I. Ikemoto *et al.*, in *Handbook of Chemistry*, 3rd ed., edited by M. Itoh (Maruzen, Tokyo, 1984), Vol. 2, Chap. 14, p. 582 (in Japanese).